Modelling Time Reversal Applications in a Reverberation Chamber using the Current Image Method

Maxime Spirlet*, Valéry Broun†, Philippe Camus†,
Christophe Geuzaine‡, Véronique Beauvois‡ and Isabel Molenberg‡

* CECOTEPE, Research Center, maxime.spirlet@hepl.be,
Quai Gloesener 6, 4020 Liège, Belgium,
† Haute Ecole de la Province de Liège (HEPL), Engineering Department, Electronics Service,
Quai Gloesener 6, 4020 Liège, Belgium,
‡ Université de Liège (ULg), Applied & Computational Electromagnetics,
B28 Institut Montefiore, 4000 Liège, Belgium.

***Abstract*—In this paper, we present a numerical model to analyze Time Reversal applications in a reverberation chamber using the current image method. The principles behind this numerical model are presented in the first part of the paper. The major advantage of this reverberation chamber model is that it requires a lot less computing time than usual solvers with qualitatively satisfying results. Next, an extension of our method to model Time Reversal Mirrors in reverberating cavities is described. Finally, two examples of Time Reversal refocusing using Time Reversal Mirrors of one or several elements are presented for illustration.**

I. Introduction

CECOTEPE in collaboration with ULg is interested in finding alternatives to measurements in anechoic chambers. Indeed, these are often too expansive or too cumbersome for non commercial use, while mandatory for many EMC measurements. Furthermore, for large object under test, the fixed dimensions of the chamber might be considered as a limitation. To overcome those limitations, we would like to develop a system that could be used in a non anechoic environment so that it would behave as an anechoic room for EMC measurements (emission, antenna characterization,...). In particular, reflections caused by non absorbant walls, the floor and the ceiling should be suppressed. To achieve this, we have first considered a highly reverberant but noise-free environment: the reverberation chamber (RC).

Time Reversal techniques were chosen in order to take advantage of the undesired reflections to approach the conditions of anechoic chambers. Although the technique is quite easy to implement, some specific and expensive equipment is required. We hope that within a few years the cost of such equipment will be significantly decreased. It is also hoped that in the meantime, more knowledge will be gained and that an improved model will be designed.

The behavior of the RC has been studied both experimentally and numerically using simulation models. However, usual electromagnetic solvers may require long computing times for large cavities. We have therefore developed a faster software especially designed for the simulation of the propagation of waves inside a cavity.

In the first part of this paper, we present the numerical model and some theoretical considerations upon which the software is based.

In the second part of the paper, we present our first results obtained using the Time Reversal model.

II. Numerical model

Our model is based on the current image (CI) theory used to model the reflections inside the cavity [1]–[3]. The principles of this theory and its extension to a cavity are described as follows:

Considering a current vector I in the neighbourhood of a perfect electric conductor (PEC), respecting the boundary conditions, the current vector and the PEC can be equivalently replaced by the same current vector and another vector I' on the other side of the PEC plane. The direction of the normal component of the current I' is same as that of I while the direction of the tangential component is opposite to that of I as illustrated in Fig. 1.

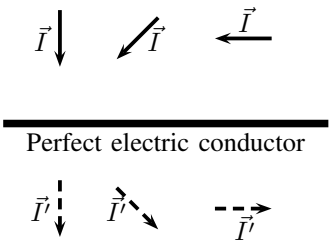

Fig. 1. Illustration of the images from current vectors near a Perfect Electric Conductor.

In a 2D rectangular (3D parallelepipedic) ideal cavity there are 4 (6) PEC planes. Therefore, the case of a current I

inside a cavity is equivalent to replacing the 4 (6) walls by the same number of current images. This corresponds to the first reflection. The reflected current is then again reflected by another wall. This second reflection is, in turn, replaced by 4 (6) new current images for each of the previous 4 (6) images. In theory, the next reflections should also be replaced using the same technique and this should be repeated an infinite number of times.

The order of the cavity n is defined as the number of reflections considered. The reflections are related to their image currents using this order n. The combination of all the current images finally yields a pattern like the one illustrated in Fig. 2 for a 2D rectangular cavity. The same kind of pattern could be observed in a 3D parallelepipedic cavity with extra currents in the third dimension.

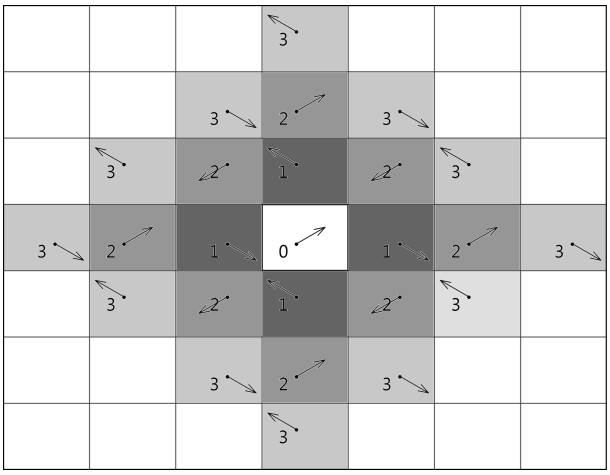

Fig. 2. Positions and directions of the generated current images up to the third order inside a 2D cavity.

The losses due to the RC walls are introduced using a reflection coefficient R [2]. After each reflection the signal amplitude is decreased. The image current of order n is defined by

$$I_n = I_0 R^n \quad \text{with} \quad 0 < R < 1 \tag{1}$$

where I_0 is the source current.

The value of R can be determined experimentally [2] from the time constant τ of the RC and then using the formula

$$R \approx e^{-\frac{L}{2c\tau}} \tag{2}$$

where c is the speed of light and L is the mean distance between two successive reflections.

Rigorously, the reflection coefficient R depends on the frequency and should be determined for the complete range of usable frequencies. Experimental values of R as a function of frequency are shown in Fig. 3. Those results were obtained using the unloaded RC of ULg. Those values have been obtained at a specific location inside the unloaded chamber and the mean value could be refined by repeating the measurements at multiple test points inside the volume. It should be noted that a global mean value of R is acceptable here, as it does not modify our model qualitatively.

The experimental value of R represents the losses of the walls of the RC but also all other losses that might occur inside the RC (e.g. those of the object under test, antennas, cables,...). The loading of the RC could therefore be taken into account when evaluating R.

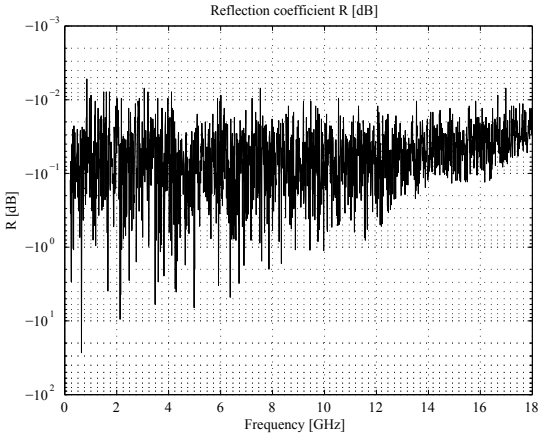

Fig. 3. Experimental values of the reflection coefficient R from measurements in the unlodaed RC of ULg.

Once the current images have been determined, the pulse response at any non particular point of the cavity can be calculated. The cavity pulse response h at a given point p is obtained by summing all radiation contributions at that point due to a synchronous current pulse excitation in each image cavity. For each image current the propagation time t to reach p can be calculated for that contribution, knowing the distance between p and the point of origin of the pulse. Finally, the contributions are sorted in chronological order after discretizing t at the desired sampling frequency.

The propagation of the source pulse excitation can be modelled using virtual antennas having an adequate radiation pattern. Virtual antennas have been introduced to improve the flexibility of the model. They can be used to avoid hard-coded equations inside the program. This way, all the information about the antenna is stored in an external file. The radiation of the source is modelled by radiation pattern from an electromagnetic solver or is user defined.

In practice, a finite number of reflections must be considered. Our criterion is based on the remaining energy inside the cavity. With $0 < R < 1$, each order brings less and less energy compared to previous ones. The reflection expansion is stopped after the marginal energy in the pulse response at order n falls behind a predefined threshold T (typically -40dB) compared to the total energy from orders 0 to $n-1$

$$E_n^{[dB]} - E_{0\to n-1}^{[dB]} \leq T^{[dB]} \tag{3}$$

Once the pulse response is known from one point to another in the cavity, it is easy to calculate the response to any input signal by convolution. The source signal $s[n]$ is convolved with the pulse response $h[n]$ to produce the signal response

$y[n]$:

$$y[n] = s[n] \star h[n] \tag{4}$$

An example of pulse response is shown in Fig. 4. The exponential decay envelope is clearly visible.

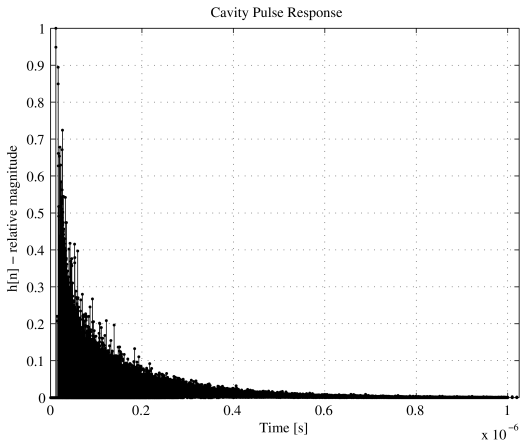

Fig. 4. Example of a cavity pulse response ($h[n]$) given by our numerical model.

III. Time Reversal

Time Reversal (TR) is a technique that allows time and space energy refocusing thanks to the reciprocity of the wave equations. Time Reversal theory is discussed in details in [4]–[6], dealing in particular with Maxwell's equations. We summarize the principle of TR hereafter. We consider a source of emission located at a point o, belonging to a volume V bordered by a closed surface S. The volume V is constituted by a reciprocal media, as shown in Fig. 5. The theoretical TR operation is performed in a four step operation :

1) The source located in o radiates in the volume V after being excited by a current density $\vec{J}$,
2) The electromagnetic wave that reaches the surface S is recorded in order to be time reversed,
3) The surface S releases the reversed electromagnetic wave,
4) The released electromagnetic wave refocuses on the point o, like an image of the reversed current density $\vec{J}$.

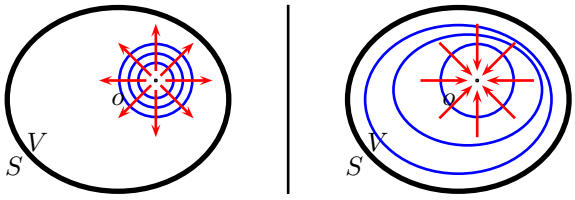

Fig. 5. Illustration of the theoretical Time Reversal principle. On the left, the source o has emited a wave. On the right, the wave that has reached the surface S is returned and reemited to be refocused on the point of origin o.

Theoretically, the surface S has to allow the recording of the received signal, its reversal and reemission at any point. But in practice, the surface S must be discretized. In the current paper, we are particularly interested in electromagnetic TR in reverberating environment. A multipath environment reduces significantly the number of points needed for the discretization of S without loosing much accuracy in the refocusing [6] (one element might already be sufficient if a wideband signal is considered). We adopt here a system-oriented approach in adequacy with the numerical model previously described, using pulse impulse responses. We define hereafter the steps of a Time Reversal operation in a cavity, where S is discretized by one element. If a signal $s(t)$ is injected at a point A in the cavity, at some recording point B in the cavity a signal $p(t)$ is received

$$p(t) = s(t) \star h_{AB}(t) \tag{5}$$

with $h_{AB}(t)$ the pulse response of the channel between A and B. Reversing the signal $p(t)$ and reemitting it in the cavity will lead at the point of origin A

$$\begin{aligned} r(t) &= p(-t) \star h_{BA}(t) \\ &= (s(-t) \star h_{AB}(-t)) \star h_{BA}(t) \\ &= s(-t) \star (h_{AB}(-t) \star h_{BA}(t)) \\ &= s(-t) \star \gamma_{AB}(t) \end{aligned} \tag{6}$$

Because of the principle of reciprocity $h_{AB}(\pm t) = h_{BA}(\pm t)$. The function $\gamma_{AB}(t)$ is the autocorrelation function of the impulse response between A and B. If $\gamma_{AB}(t) = \delta(t)$, where $\delta(t)$ is the Dirac delta function, the reversed signal $s(-t)$ and the received signal at the point of origin $r(t)$ will be equivalent: a perfect refocusing to A will occur. The term retro-propagation is intentionally avoided here as it does not really match reality [7]. The condition $\gamma_{AB}(t) = \delta(t)$ can be approximated by increasing the number of recorders or also by mixing using reverberating environments, virtually increasing the number of receivers.

A Time Reversal Mirror (TRM) is a set of one or many elements that record, reverse and reemit any received signals individually. Using a TRM with many elements increases theoretically the quality of the refocusing. But the geometry must be well chosen in order to optimize the performance of the TRM. One of the objectives of our model development is to investigate the exact influence of the TRM geometry.

Time Reversal is directly implemented using our model which is based on a discrete version of the impulse response used in equation (6). This model is particularly well suited to fast implementation of TR in RC. It can be used with TRM containing one or several elements.

IV. Applications

We carried out several comparisons between the results given by our model and those obtained using an electromagnetic solver based on Discontinuous Galerkin (DG) method. The DG code is developed in collaboration between the University of Liège and the Université Catholique de Louvain. In [8], we published results for the configuration of 3 in-plane dipoles excited by a wideband gaussian pulse inside a 2D

cavity. The normalized computed electric field is shown in Fig. 6. We have computed the expression of the error integrated over time for 3 points of interest using:

$$E_p = \frac{\sum_{t=0}^{T-1} \left|E_p^{CI}[t]\right|^2 - \left|E_p^{DG}[t]\right|^2}{\sum_{t=0}^{T-1} \left|E_p^{DG}[t]\right|^2} \quad (7)$$

with $E_p^{CI}[t]$, $E_p^{DG}[t]$ the normalized electric fields at the point p at time t for the CI method and DG method respectively. The error expressed in percent is plotted in Fig. 7. The relative error can be significant locally, especially at the edges of the wave fronts, but the pattern is not qualitatively altered.

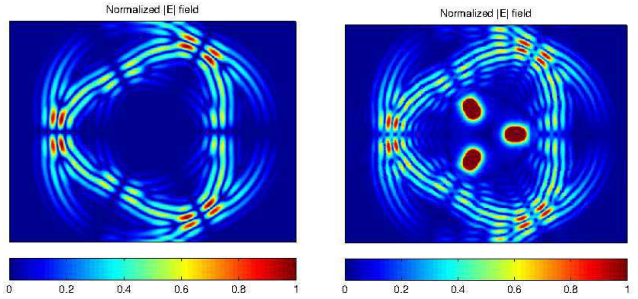

(a) CI (b) DG

Fig. 6. Normalized magnitude of the electric field with CI method (a) and DG method (b) for 3 dipoles radiating inside a 2D cavity. The source signal is a 500 MHz bandwidth gaussian pulse with 1 GHz center frequency.

An example of TR refocusing is shown in Fig. 8. This is the signal received at the point of origin after TR for the configuration illustrated in Fig. 9. The lower left patch antenna is excited by a gaussian pulse with 1 GHz center frequency and 500 MHz bandwidth. The upper right patch antenna collects the received signal and reemits the reversed signal. The magnitude of the electric field in the cavity at the refocusing time is shown in Fig. 9.

An example of TR using 14 elements TRM is shown in Fig. 10; The received signal at the point of origin after TR is plotted over time. The patch antenna in the center of the cavity is the source and is excited by a gaussian pulse with 1 GHz center frequency (500 MHz bandwidth) while fourteen isotropic antennas reemit the received signal in the cavity (the setup is detailed in Fig. 11). The magnitude of the electric field in the cavity at refocusing time is shown in Fig. 12.

V. Discussion

As shown in Fig. 7, our model is more accurate in the far-field region of the antennas than in the near-field. This was expected since we used the far-field radiation pattern of the virtual antennas in our simulation. The difference may also be amplified because no antenna coupling is considered in the model. This decreased accuracy is compensated by a significantly shorter computation time: in a typical case, the CI method is about one order of magnitude faster than the DG simulation. Considering 3D RC numerical models, the CI method should be even more interesting compared to the DG simulation.

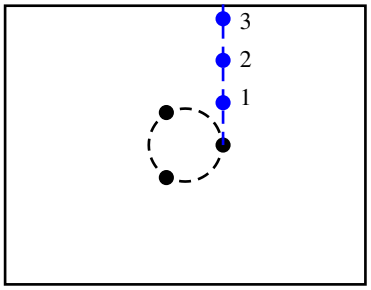

(a) Locations of the points of interest

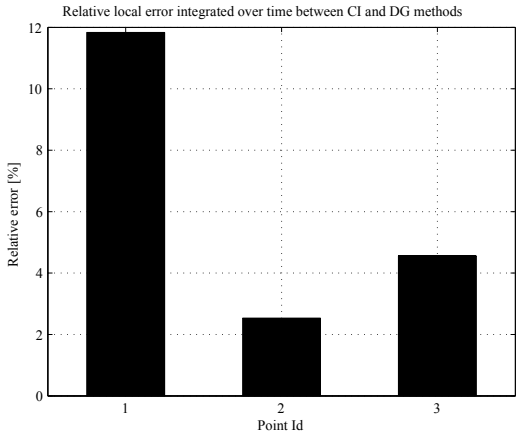

(b) Relative error at the points of interest

Fig. 7. Relative error in percent according (7) at 3 points of interest for 3 dipoles radiating inside a 2D cavity. The source signal is a 500 MHz bandwidth gaussian pulse with 1 GHz center frequency.

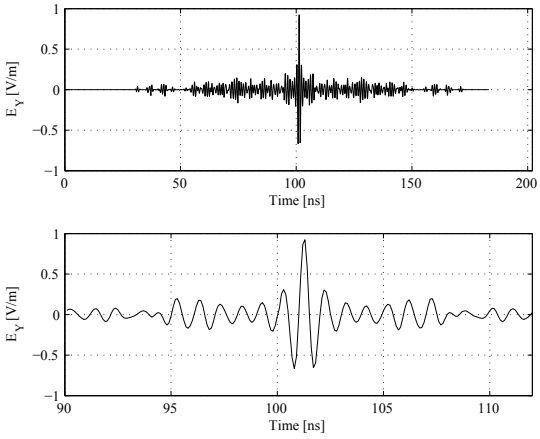

Fig. 8. Refocused signal recorded at the point of origin using a TRM of 1 element (top). The received signal is an image of the original signal reversed (gaussian pulse) and enlarged view of the pulse (bottom).

We considered a RC without the presence of any stirrer, while the RC at ULg is a mode stirred RC. Because of this, the comparison between laboratory and model is difficult. We have therefore chosen to compare our model with another numerical model instead of experimental results. If we had considered applications involving mechanical stirring, although taking

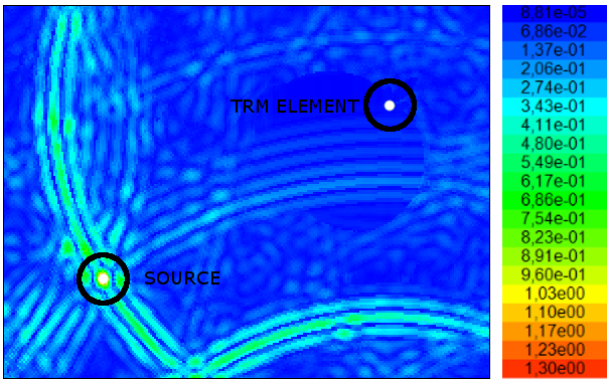

Fig. 9. TR operation using a TRM of 1 element at the refocusing instant. The magnitude of the electric field is displayed (in V/m).

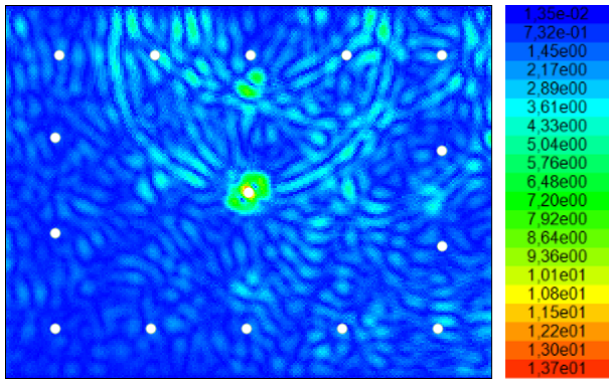

Fig. 12. TR operation using a TRM of 14 elements at the refocusing instant. The magnitude of the electric field is displayed (in V/m).

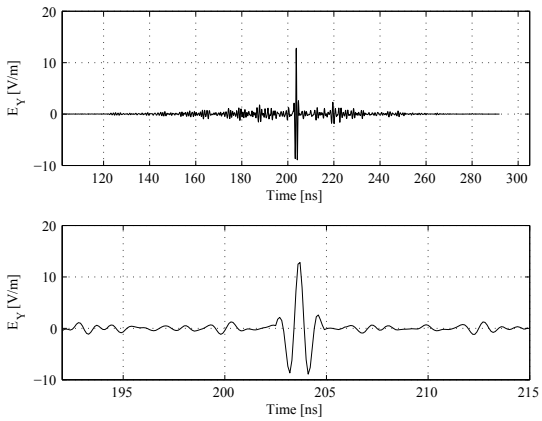

Fig. 10. Refocused signal recorded at the point of origin using a TRM of 14 elements (top). The received signal is an image of the original signal reversed (gaussian pulse) and enlarged view of the pulse (bottom).

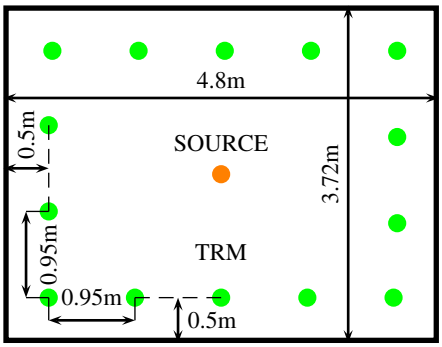

Fig. 11. TR application setup with a 14 elements TRM.

into account the stirring process is not possible with the CI method, it could be replaced by spatial or electronic stirring (even if these are less efficient). Numerically we could even modify the cavity dimensions to replace the mechanical stirrer but this has not been tested yet.

The aim of the selected TR examples shown is to essentially illustrate the feasibility of Time Reversal using the current image method. In Fig. 8 and Fig. 10, the time of refocusing is visible at $t \approx 101$ ns and $t \approx 204$ ns respectively: we retrieve an image of the original gaussian pulse. We also observed that the amplitude of the refocusing is higher for the 14 elements TRM than with the 1 element TRM. Each element of the TRM contributes to the refocusing, making the refocused signal amplitude at the source higher than for a single element TRM. Fig. 9 and Fig. 12 illustrate that energy is mainly localized at the point of origin in both cases. Those examples also confirm that TR method can still be applied inside a cavity with low losses (R), as discussed in [9].

This model is currently being used to study the impact of the geometry as well as the impact of the number of elements in the TRM. This should be helpful to better place the TRM elements once measurements are carried out.

VI. Conclusions

We have developed a numerical model of reverberation chamber in pulsed domain using the current image method. We have shown that our model provides qualitatively satisfying results in the far-field region and is much faster than existing electromagnetic solvers in this particular case. We have also extended this model and developed a set of tools for Time Reversal applications in reverberation chambers. We have shown that the Time Reversal operation can be used with our model but it is still being optimized and improved. Using this model, we are now ready to develop new and more complex Time Reversal applications that could be subsequently used in practice.

Acknowledgment

This research was funded by a FIRST grant of the Walloon Region (DGO6).

REFERENCES

[1] E. Amador, C. Lemoine, P. Besnier, and A. Laisné, "Studying the pulse regime in a reverberation chamber with a model based on image theory," in *Electromagnetic Compatibility (EMC), 2010 IEEE International Symposium on*, july 2010, pp. 520 –525.

[2] E. Amador, "Modèles de compréhension par la théorie des images des phénomènes transitoires et du régime permanent en chambre réverbérante électromagnétique," Oct. 2011, d11-23. [Online]. Available: http://tel.archives-ouvertes.fr/tel-00652164

[3] E. Amador, C. Lemoine, P. Besnier, and A. Laisné, "Reverberation chamber modeling based on image theory: Investigation in the pulse regime," *Electromagnetic Compatibility, IEEE Transactions on*, vol. 52, no. 4, pp. 778 –789, nov. 2010.

[4] J. de Rosny, G. Lerosey, and M. Fink, "Theory of electromagnetic time-reversal mirrors," *Antennas and Propagation, IEEE Transactions on*, vol. 58, no. 10, pp. 3139 –3149, oct. 2010.

[5] G. Lerosey, "Retournement temporel d'ondes électromagnétiques et application à la télécommunication en milieux complexes," Dec. 2006. [Online]. Available: http://pastel.archives-ouvertes.fr/pastel-00003585

[6] G. Lerosey, J. De Rosny, A. Tourin, A. Derode, G. Montaldo, and M. Fink, "Time reversal of electromagnetic waves." *Phys Rev Lett*, vol. 92, no. 19, p. 193904, 2004.

[7] W. Dyab, T. Sarkar, and M. Salazar-Palma, "Antenna reciprocity and the theory of electromagnetic time reversal," in *Antennas and Propagation Society International Symposium (APSURSI), 2012 IEEE*, july 2012, pp. 1 –2.

[8] M. Spirlet, V. Broun, P. Camus, and V. Beauvois, "Modelling of a reverberation chamber using current image method."

[9] M. Davy, J. de Rosny, and M. Fink, "Focusing and amplification of electromagnetic waves by time-reversal in an leaky reverberation chamber," in *Antennas and Propagation Society International Symposium, 2009. APSURSI '09. IEEE*, 2009, pp. 1–4.